Elnaz Shahbazali¹ / Volker Hessel¹ / Timothy Noël¹ / Qi Wang¹

Metallic nanoparticles made in flow and their catalytic applications in micro-flow reactors for organic synthesis

¹ Laboratory of Chemical Reactor Engineering/Micro Flow Chemistry and Process Technology, Department of Chemical Engineering and Chemistry, Eindhoven University of Technology, P.O. Box 513, 5600 MB Eindhoven, The Netherlands, E-mail: e.shahbazali@tue.nl, v.hessel@tue.nl, t.noel@tue.nl, q.wangt@tue.nl

DOI: 10.1515/psr-2015-0016

1 Introduction

Recently, nanoparticles, of spherical and non-spherical shape, have been used widely in many different areas such as electronics, energy, textiles, biotechnology, etc. [1–6]. Such increasing application of nanoparticles leads to an increasing focus on studying the way nanoparticles are synthesized. Conventionally, nanoparticles are produced with methods such as liquid-phase synthesis, e.g. via co-precipitation of soluble products, sol-gel process, microemulsions, etc. [7–10], which are applied mostly in traditional batch processes. One of the drawbacks of the conventional methods is the lack of suitable control over mixing. Bad mixing creates particles with a broad size distribution, irreproducibility of size and morphology. Besides, it is difficult to obtain the same result when scaling up the batch process, i.e. to achieve process reliability.

Currently, microfluidic technology has been introducing a new method to over-come conventional process limitations [11-14]. The high surface area to volume ratio and reduced diffusional dimensions characterize microfluidic devices and enable, among other advantages, more controlled transport such as mass and heat transfer as well as reducing chemical reaction time. The advantages from the increased heat transfer rates can be very important for instance in multiphase reactors, where the improved heat transfer in microreactors diminishes the chance of the formation of the so-called local "hot-spots", compared to batch reactors. Accordingly, the product selectivity is improved by performing exothermic, multiphase reactions in a microreactor. Furthermore, the small-sized microreactors have safety advantages in the use of toxic, harmful or expensive chemicals. In addition, microfluidic synthesis techniques operate at a steady state and give superior control over reaction conditions, such as reagent addition, mixing and temperature. Also, scaling up is more efficient than for a batch process [15, 16]. Regarding the scale up and flow pattern, mixing in flow systems is relatively well characterized in comparison to batch vessels. Therefore, scaling up the flow reactors is easier and faster. Another interesting feature is that online monitoring can be implemented, allowing quick parameter-space study for kinetic studies and yield optimization [17, 18]. These advantages are key to producing a wide range of nanoparticles with more uniform size distribution and desired shape, morphology, (super-)structure and crystallinity [13] (Table 1 presents a summary of the comparison of the main features of the nanoparticle synthesis for batch and flow).

Table 1 Comparison of the main features of the nanoparticle synthesis for batch and flow [11–18].

	Batch	Flow	
Minimal particle size	small	very small	
Particle size distribution	large	small	
Reproducibility	poor to moderate	good to very good	
Operational stability (e.g. fouling)	very good	good	
Mixing quality	good	very good	
Surface area to volume ratio	small	high	
Mass and heat transfer	moderate	very good	
Scale-up efficiency	good	very good	

Volker Hessel is the corresponding author.
© 2016 Walter de Gruyter GmbH, Berlin/Boston.
This content is free.

As mentioned, frequently all types of nanoparticles including inorganic [19], organic [20] and polymeric [21] ones with well-defined composition have been synthesized within microreactors. Inorganic nanoparticles are classified in three categories, dielectric [22, 23], semiconductor [24, 25], and metal [26, 27] nanoparticles. Considering metal nanoparticles, they can be applied as a catalyst in catalytic reactions.

The complexity of the nanoparticle synthesis with its cascade of elemental reaction steps – e.g. reduction, seed formation, growth and stabilization – is increasingly reflected in a complexity of the microfluidic system. Separate feeds for the respective reactants and stabilizers are given, each elementary step has its own reaction channel and is operated at the best process conditions for the given step. Thus, the microfluidic architecture is characterized by a series of mixing injections and reaction channels (Figure 1). Some of these devices shown in Figure 1 were used in the examples described in this review.

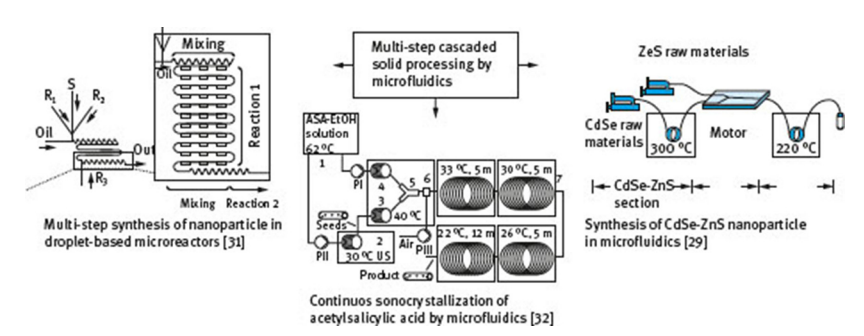


Figure 1: Metal nanoparticles formation and application by microfluidics (Reprinted with permission from [32]. Copyright (2004) American Chemical Society and The Royal Society of Chemistry [29, 31]).

Therefore, in this chapter, it is planned to briefly review the recent research on selected metal nanoparticles (gold, silver, palladium, platinum, copper) synthesis and their catalytic applications in organic reactions in microfluidic devices. The most recent progress on the synthesis of some more industrially important noble metal nanoparticles is discussed, providing some examples from each one.

2 Metal nanoparticles in a microfluidic reactor

Metal nanoparticle formation involves at least three steps: an initial chemical reaction step leading to nucleation, and subsequent particle growth (sometimes followed by polymer stabilization). In most conventional methods, both processes take place simultaneously in a one-pot process under reaction conditions that are often not optimal for both. These processes also take place under mixing-masked conditions due to the speed of this elementary process. Therefore, synthesized particles in batch often suffer from broad size distribution [33]. In order to obtain uniform nanoparticles, all nucleation processes should take place in a short period of time (no longer than needed) and separately (each process under optimal conditions). Materials should be supplied slowly so as not to reach the concentration level at which nucleation would occur. The goal is rather to prepare many nucleation centers so that small particles are produced. Because of the better control of the reaction's kinetic parameters, such as better mixing and efficient heat and mass transfer, microfluidic reactors have been widely designed and applied to produce uniform metal nanoparticles. For metal nanoparticle synthesis, the benefits of using microreactors over conventional methods rely on the very fast mixing, the capability to control the temperature along the flow and the potential to combine separated reaction steps in a one-flow [14].

2.1 Gold

2.1.1 Synthesis

Gold nanoparticles have attracted significant attention due to their wide range of applications. For a more detailed overview of gold nanoparticle applications in chemistry and bioscience, the reader is referred to a comprehensive review of this topic [34].

As one of the first works, the synthesis of gold nanoparticles in microfluidics was reported by Wagner $et\ al.$ [26]. Single-phase flow [13] is applied to synthesize gold nanoparticles (5 to 50 nm) in a glass-silicon microreactor directly from a gold salt (HAuCl₄) and a reducing agent (ascorbic acid). By optimizing the experimental parameters such as flow rate, pH and excess of reducing agent, a narrow size distribution is achieved which is

two times narrower than in a conventional synthesis. Moreover, by elevating pH during the reaction and hydrophobization of internal reactor surfaces, reactor fouling was decreased [26]. The higher the pH, the smaller mean diameter was obtained (at pH = 2.8, the mean diameter = 21 nm and at pH = 9.5 the mean diameter = 8 nm). The same authors used a microfluidic chip, a three-step static micromixer (by IPHT Jena). This device contains four fluid inlet ports and one outlet port. In the first step, the first two inlets are premixed. Then in the second step, the third inlet is premixed with the mixture of the first inlets. Finally, the last inlet is mixed with the mixture stream of previous inlets. For a single mixing step in the chip device, the residence time was varied from about 1 second to 1 minute. This lead to the formation of Au nanoparticles in single and cluster forms with different shapes such as hexagonal nanocrystallites or tetrahedron-like cluster of nanoparticles (Figure 2) [35].

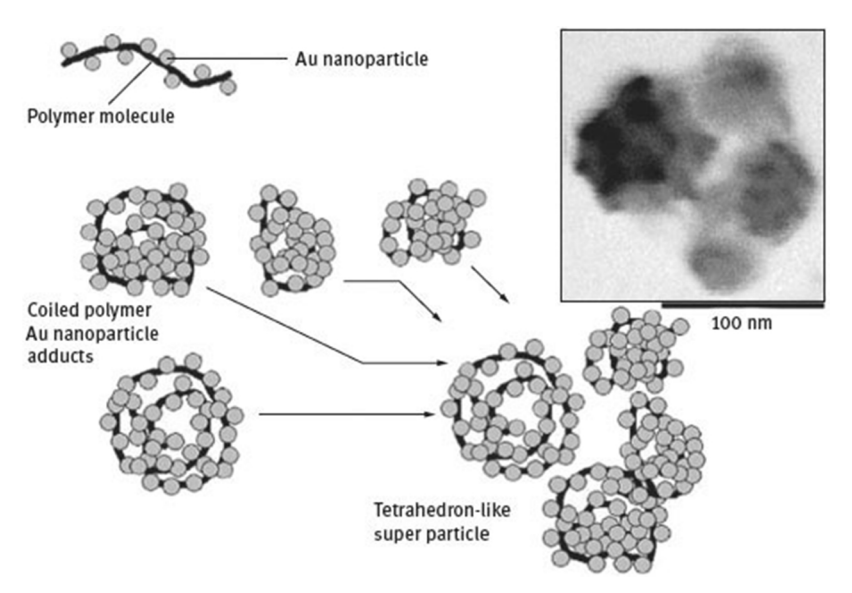
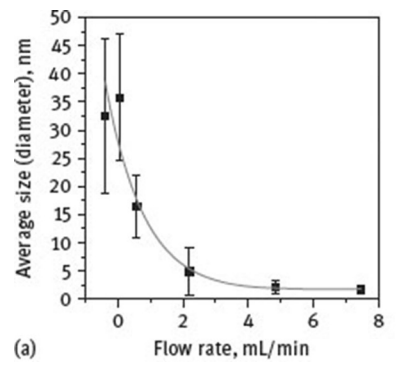


Figure 2: Pictorial representation of proposed scheme for the formation of tetrahedron-like super-clusters of Au nanoparticles during the micro-flow-through experiment (reproduced by permission of The Royal Society of Chemistry) [35].

Luty-Blocho *et al.* [36] investigated gold nanoparticle synthesis in continuous flow using a fast reducing agent, sodium borohydride, which needed even faster mixing. The whole idea was to chemically impact the nucleation and growth processes in order to get smaller and better-defined nanoparticles (this was seen under the umbrella of the Novel Process Windows concept). A slow reducing agent, ascorbic acid, was investigated to compare to the fast one. In this sense, the impact of process conditions on each elementary step such as mixing and reaction was varied; e.g. using two polymers of known fast and slow particle absorption. A multilamination micromixer was utilized, which can mix in some 10 ms, depending on the flow rates. When reducing slowly the gold particle precursor HAuCl₄ with ascorbic acid, the smallest nanoparticles (0.8–4 nm) are obtained for the highest applied flow rate of 7.5 ml/min (Figure 3 (a)). Using the fast reducer, sodium borohydride, even smaller nanoparticles (0.6–3 nm) are achieved for the flow rate of 10.0 ml/min. In the batch process, the average size and particle size distribution is broader (1.5 nm–2 μ m) (Figure 3 (b)). Thus, when comparing two reducing agents, the gold nanoparticles that were synthesized through sodium borohydride are smaller and more uniform. This demonstrates that mastered chemical conditions supported by the microfluidics engineering can allow a certain nanomaterial shaping control.



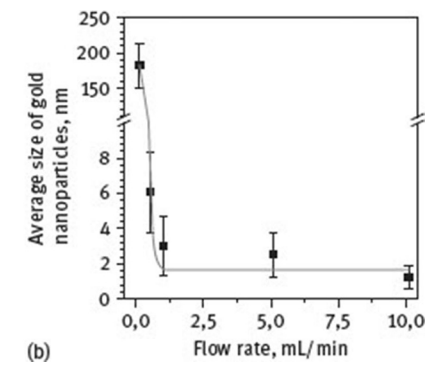


Figure 3: Flow rate influence on the average size of gold nanoparticles synthesized through micro processing for (a) ascorbic acid as slow reducer and (b) sodium borohydride as fast reducer (reproduced by permission of Elsevier BV) [36].

Paclawski *et al.* [28] produced gold nanoparticles by reduction of gold (III) chloride complex ions using glucose as a reducing agent in a microreactor. This process includes a series of elementary steps: (a) reduction of gold(III) and gold(I) complex ions ([AuCl3(OH)] –) to metallic gold; (b) nucleation; and (c) growth of gold nanoparticles. The synthesis was performed in the presence of different amounts of polyvinylpyrrolidone (PVP) as a stabilizing agent. In these studies, the rate constant is determined from experiments done in a batch system. Then, based on information obtained from experiments in the batch reactor (the rate law as well as the optimal PVP concentration), gold nanoparticles were synthesized at different flow rates of the stabilizer solution (0.05–1.45 ml/min) and of the gold precursor and glucose mixture (3.0 ml/min). In the studied system, glucose also acts as a capping agent. However, because of the high rate of the nanoparticle formation, glucose is not found to be an efficient stabilizer. The addition of PVP into reaction mixtures increases the stability of gold nanoparticles and enables one to obtain smaller nanoparticles. In this system, the diameter of synthesized spherical gold nanoparticles can be controlled from 10 to 50 nm.

By using segmented flow technique [37] in microflow reactors instead of a single-phase flow, gold nanoparticles of even better defined properties are produced [38]. In the segmented flow technique, an immiscible fluid is introduced to divide the reagent phase into discrete slugs or droplets. The key advantages of segmented flow include the reduction of axial dispersion and susceptibility to reactor fouling [37]. Based on the analysis of flow fields and the resulting particle size distribution, Cabeza *et al.* illustrated that the slip velocity between the two fluids and the internal mixing in the continuous-phase slugs determines the particle size distribution [38]. The reduction in the axial dispersion has less impact on the particle growth and hence on the particle size distribution. Gold nanoparticles are synthesized from HAuCl₄ with rapid reduction by NaBH₄ (Figure 4). In this way, gold nuclei are obtained, which grow by agglomeration, and it is controlled by the interaction of the nuclei with local flow. Therefore, the difference in the physical properties of the two phases, such as density, viscosity and surface tension, and the inlet flow rates finally control the particle growth. Hence, a careful choice of continuous and dispersed phases is necessary to control the nanoparticle size and size distribution.

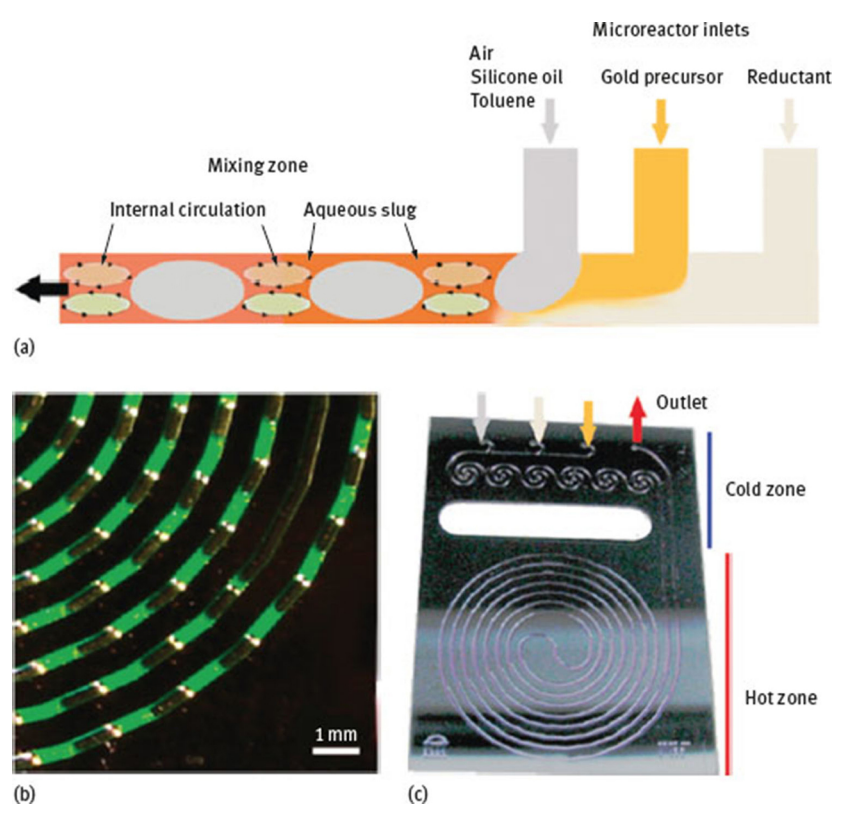


Figure 4: Pictorial representation of (a) the segmented flow in microflow reactors, (b) segmented slugs produced at residence time of 10 s, (c) spiral silicon/pyrex microreactor (400 μ m channel width and depth, 100 μ l reaction zone volume) (reprinted with permission from [38]);

By increasing the residence time, the particle size distribution widened independent of the inert fluid dispersed in the aqueous phase. For instance with toluene as the inert fluid, particle sizes of 3.8 ± 0.3 , 4.6 ± 2.1 , and 4.9 ± 3.0 nm are achieved at residence times of 10, 20, and 40 s, respectively [38].

In addition to spherical nanoparticles, anisotropic metal nanocrystals like nanorods have been synthesized using microfluidics [39–41]. As one of the early works, Boleininger *et al*. [39] presented a continuous flow synthesis of gold and silver nanorods with specific shapes. They used small, spherical gold seeds in a growth solution

containing the gold salt (HAuCl₄) in millimolar concentrations, a mild reducing agent (ascorbic acid) and a high concentration of a surfactant molecule (cetyl trimethyl ammonium bromide (CTAB)), which produces a rod-shaped anisotropic particle growth solution. The seeds and growth solution are injected to a microreactor. The effects of the concentration in the mixture of growth-to-seeds solution and of the growth temperature on particle shape were tested. Fewer seeds generate particles of higher aspect ratio and also a higher growth temperature produced smaller aspect ratio (fatter rods) (Figure 5).

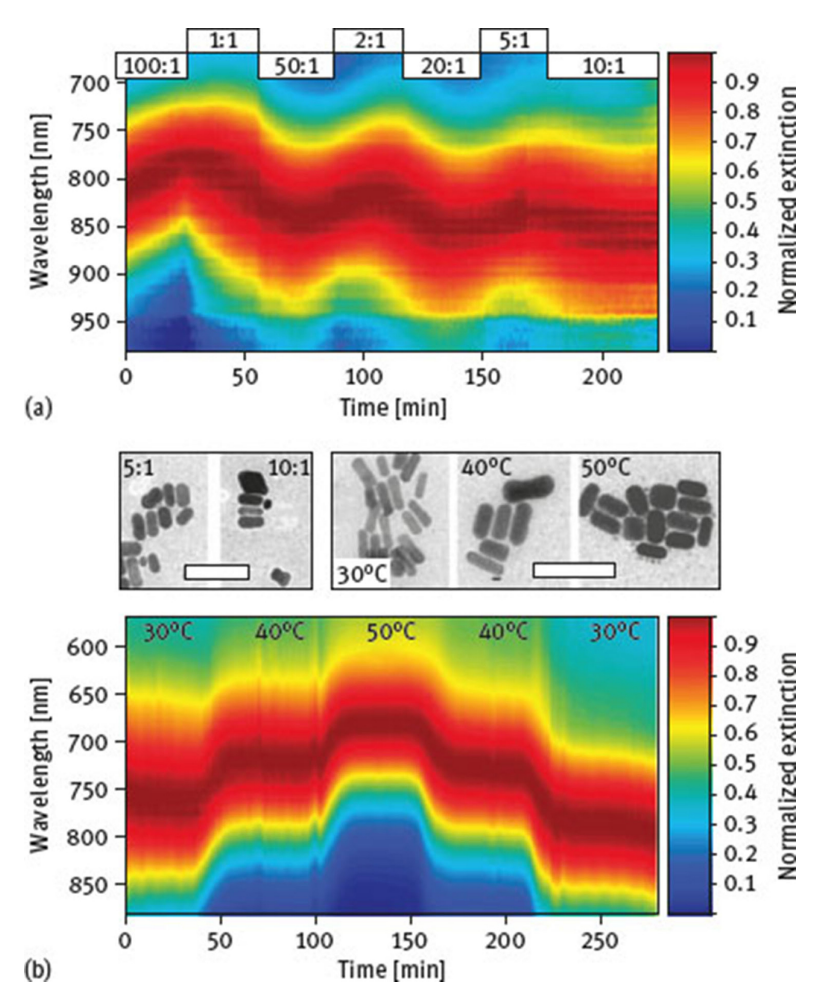


Figure 5: Pictorial representation of the measured extinction, which is color-coded as a function of time. (a) The ratio of growth-to-seed solution was varied from 100: 1 to 1:1. (b) Variation of the growth temperature from 30 to 50 °C (reproduced by permission of The Royal Society of Chemistry) [39].

Bullen *et al.* [40] presented a direct seedless approach to synthesize gold nanorods in continuous microfluidic. Two different solutions ($HAuCl_4/CTAB/acetylacetone$ and $AgNO_3/CTAB/carbonate$ buffer) at room temperature are introduced to a rotating tube processor followed by a narrow channel processing microfluid. The rotating tube processing provides a good mixing of two solutions and therefore with the aid of centrifugal force gold nanocrystals were formed. Thereafter, the gold nanocrystal solution continuously entered the narrow channel processor for growth of the gold nanorods (Figure 6).

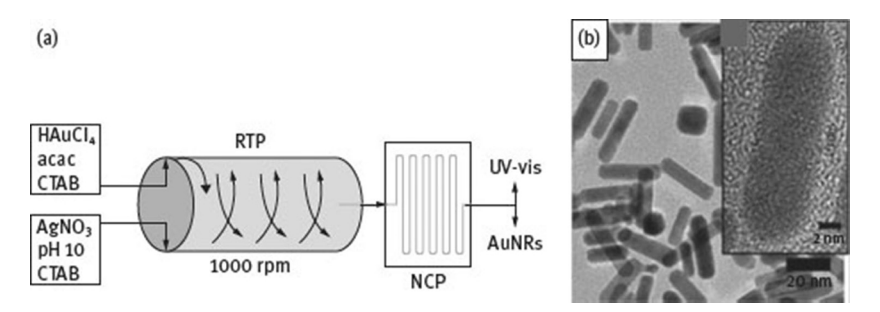


Figure 6: Pictorial representation of (a) continuous flow setup, (b) HRTEM images of gold nanorods (reproduced by permission of The Royal Society of Chemistry) [40].

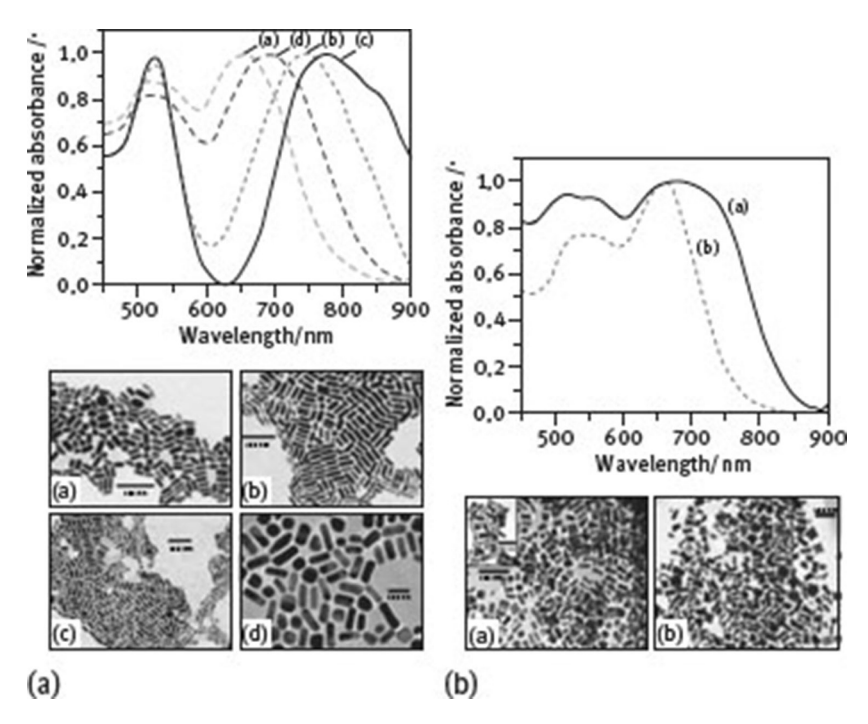


Figure 7: Pictorial representation of UV/V is absorbance spectra and TEM images of (A) spherical–spheroidal particles, $[Au^{[3+]}] = 0.6$ nM, [CTAB] = 126 mM (in reagent R_1), and [ascorbic acid] = 5.2 mM (in reagent R_2); (B) rod-shaped particles of varying aspect ratios, $[Au^{[3+]}] = 0.62$ mM, [CTAB] = 123 mM (in reagent R_1), and [ascorbic acid] = 5.2 mM (in reagent R_2); (reproduced by permission of Wiley-VCH, Weinheim) [41].

In addition to single-phase flow, droplet-based flow has been used to synthesize anisotropic gold nanocrystals. Duraiswamy $et\ al.\ [41]$ used presynthesized gold nanoparticle seeds and growth reagents. A first reagent solution contained a premixed Au^{3+} , Ag^+ , and CTAB solution; a second reagent solution contained an aqueous solution of ascorbic acid. These are dispensed into monodisperse picoliter droplets which are produced by a microfluidic T-junction. From the other arm of the T-junction, silicon oil was continuously introduced into the microchannel. Creating the mixtures in a droplet prevents the contact between the growing nanocrystals and the microchannel walls.

The effects of the reagent concentrations and of the flow rate ratio of the oil to aqueous reagent streams were studied. By varying those critical factors, nanocrystals with desired shapes and sizes with tunable optical resonances are achieved.

Regarding the scale-up concept of the nanoparticle synthesis in microfluidics, Gomez *et al.* have presented a scaled-up production of high-quality plasmonic hollow gold nanoparticles for the first time [42]. The process was designed with a scale up factor of 10 (Figure 8). It was reported that gold nanoparticles were functionalized with polyethylene glycol and sterilized in microfluidics. So, with the aid of microfluidic system, the on-line implementation of two new stages, surface functionalization and sterilization, in nanoparticle synthesis was possible.

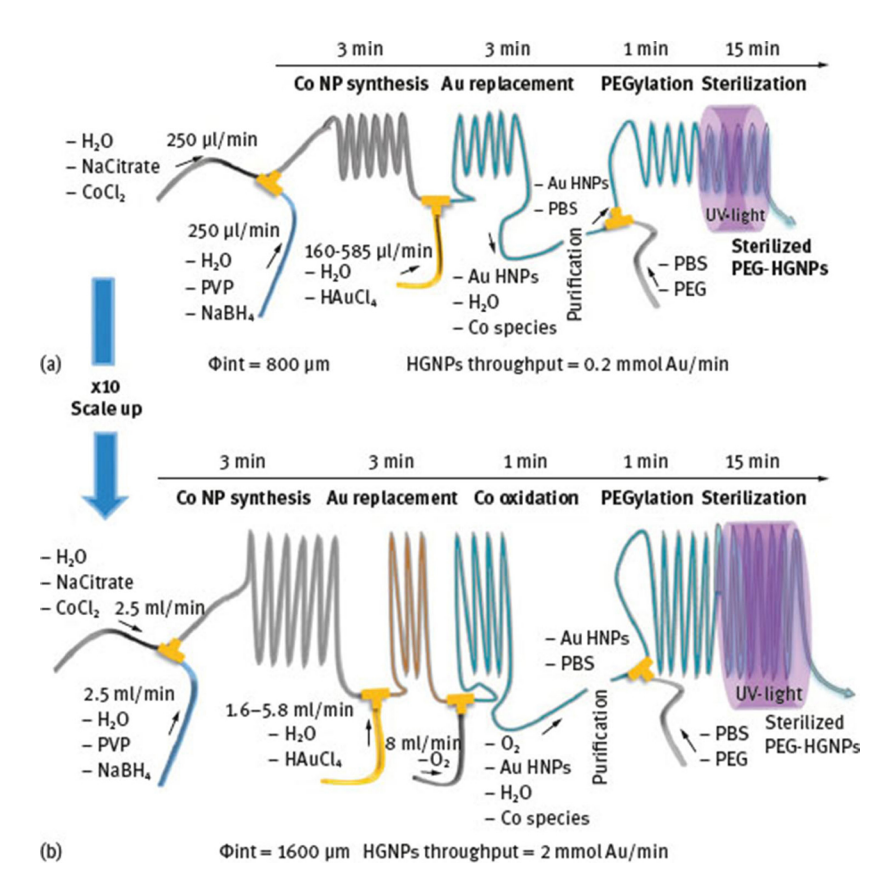


Figure 8: Comparison of experimental set-up (A) and scaled up set-up (B) to produce hollow gold nanoparticles: (A) reactor dimensions: inner diameter = $800 \, \mu m$, length = $913 \, cm$; (B) reactor dimensions: inner diameter = $1600 \, \mu m$, length = $3088 \, cm$ (reproduced by permission of The Royal Society of Chemistry) [42].

2.1.2 Applications

One of the recent applications of gold nanoparticles in flow chemistry is catalyzing the aminoalkylation reaction [43]. Abahmane $\it et al.$ studied the A^3 -coupling (alkyne, aldehyde, amine) reaction under heterogeneous catalysis in a two-step microfluidic system. The A^3 -reaction mechanism includes two reaction steps that require different catalytic supports. Montmorillonite K-10 (MM K-10) is applied to promote the initial condensation reaction and Au nanoparticles on an alumina support are used to catalyze the second aminoalkylation step.

Three different reaction regimes A–C were realized by operating at one temperature or using a two-temperature ramp as well as having different reactant insertion scheme along the reaction pathway (Figure 9). Applying reaction regime C and MM K-10 as a catalyst for the first reaction at 25 °C and 2.5% gold nanoparticles supported on Al_2O_3 as a catalyst for the second reaction at 80 °C, a conversion of 97% could be obtained. The flow-chemistry approach considerably improved the reaction performance of the A^3 coupling reaction in terms of shortened reaction time and higher yields compared with conventional batch reactors.

Figure 9: Pictorial representation of different reaction regimes A, B, C; PBCR1 (Montmorillonite K-10) and PBCR2 (Au-NP@Al₂O₃): packed-bed capillary reactors (reproduced by permission of Wiley-VCH, Weinheim) [43].

Homogeneous and heterogeneous catalysis have their own advantages and a combination of those advantages could develop sustainable catalysts with novel reactivity and selectivity. Heterogeneous catalysts are recycled more easily than homogeneous ones, but it is difficult to apply them to traditional organic reactions. As a solution out of this dilemma, Gross $et\ al.\ [44]$ replaced homogeneous $AuCl_3$ with a dendrimer encapsulated Au nanoparticle, a heterogeneous catalyst, to catalyze olefin cyclopropanation reactions. The diastereoselectivity of Au-catalysed cyclopropanation reactions can be considerably improved (Scheme 1). The same heterogeneous catalyst was also applied in a fixed-bed flow reactor. By adjusting the residence time of reactants, the catalytic reactivity and product selectivity of secondary reactions can be well controlled in a way that is not easily available to homogeneous catalysts (Scheme 2).

Figure 10: Comparison of homogeneous and heterogeneous gold catalysts for the formation of a substituted cyclopropane [44].

Figure 11: Comparison of the total conversion of gold-catalysed cyclopropanation reaction for different flow rates in batch and flow [44].

Additionally, Gómez *et al.* applied ionophore Au nanoparticles within a microfluidic system, which consists of an optical detector (UV-Vis), that selectively and continuously monitors the Hg(II) concentration [45]. Here, Au nanoparticles were introduced as optical transducers. The microfluidic system had improvements in analytical features in comparison with the batch scale, such as having a lower detection limit up to 11 ppb, lower analysis time and higher sensitivity to detect Hg over other metal ions. The detection limit and sensitivity were assessed from calibration curves at low Hg ion concentrations.

2.2 Silver

2.2.1 Synthesis

One of the earlier methods to synthesize silver nanoparticles in a microflow reactor was based on thermal reduction [27]. Lin *et al.* [27] synthesized silver nanoparticles by thermal reduction of silver pentafluoropropionate using trioctylamine (TOA) as a surfactant in isoamylether in a continuous flow tubular microreactor. A narrow particle size dispersion is obtained.

The reaction mixture is introduced into a tubular coil made of a stainless-steel needle (0.84 mm id) heated to a temperature of between 100 and 140 °C using an oil bath. The ratio of TOA/silver pentafluoropropionate, the flow rate, the temperature versus time profiles and the reaction temperature were varied to investigate their effects on the average size and distribution range of the silver nanoparticles. The flow rate has major influence on the size of the nanoparticles and their polydispersity. At a flow rate of 0.08 ml/min, the average diameter of the Ag nanoparticles was 8.7 ± 0.9 nm. As the flow rate is increased to 0.6 ml/min, the synthesized particles become polydisperse and the average diameter of nanoparticles is reduced to 5.6 ± 1.3 nm (Figure 12). In contrast, a change in the TOA concentration did not make any substantial difference in either the size or size distribution of the nanoparticles. Changing TOA/silver pentafluoropropionate molar ratios from 3, 6 to 12, silver nanoparticles are synthesized with average diameter of 8.7 ± 0.9 , 8.6 ± 0.9 , and 8.6 ± 1.0 , respectively (flow rate: 0.08 ml/min; temperature: 100 °C).

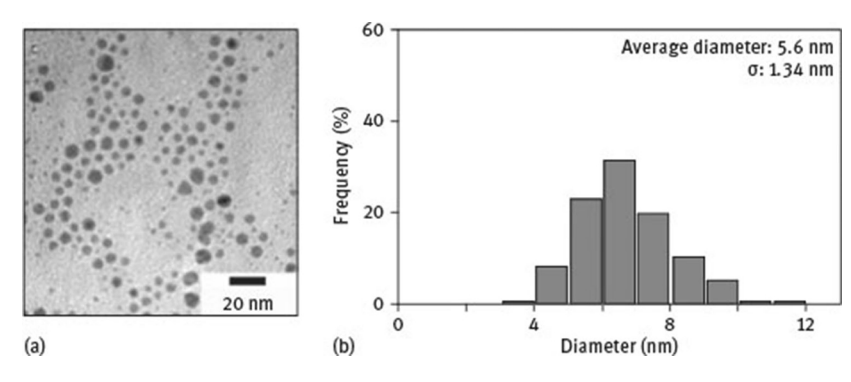


Figure 12: TEM image of the particle size distribution analysis of the Ag nanoparticles made in the tubular microreactor at a flow rate of 0.6 ml/min (reprinted with permission from [27]);

He *et al.* [46], investigated the effect of the interior wall of the capillary tube on the synthesis of silver nanoparticles and found out that the well-dispersed silver nanoparticles were synthesized continuously in a PTFE micro-capillary reactor. A relation between the particles and the interior wall of the tube results in a broader size distribution and a lower yield.

In order to observe the effect of segmented flow on the nanoparticle size distribution, Kumar *et al*. [47] applied a unidirectional expanding spiral microreactor. Stearic acid sophorolipid reduced/capped Ag nanoparticles were synthesized in the aqueous phase and air or kerosene was utilized as an inert phase to produce the gas–liquid and liquid–liquid segmented flow, respectively. While in one case the reactant phase is in the form of dispersed phase slugs, in the other it is in the form of continuous phase. The particle sizes were much smaller when generated by gas–liquid flow than by liquid–liquid flow. This effect is strengthened by the unidirectionally expanding spiral geometry of the channel, inducing transverse flows.

The effect of segmentation, which is determined by the slug sizes and the slip velocity, controlled the nanoparticle size distribution. The micromixer, which has a smaller orifice diameter, yields smaller slugs and also a narrow particle size distribution.

Knauer et~al. [48] presented a two-step micro-flow technique for colloidal dispersion synthesis of noble metal core/shell (Au/Ag) and multishell nanoparticles (Au/Ag/Au) in aqueous solute ions in the presence of CTAB.

Binary metal nanoparticles of silver and gold can have optically fine-tuned absorption in the visible spectrum, so-called plasmonic absorption. The shift of the plasmonic band is influenced by the ratio between silver and gold, the shape and the size of the binary particles, and the distribution of the two metals inside the particle. For example, when forming silver or gold as a shell or core, a different plasmon absorption results. Similar to other nanoparticle applications (such as catalysts or surface enhanced Raman spectroscopy), the surface conditions of the metal shell/core particles are of major importance [49, 50].

The synthesis is based on the reduction of a gold salt, $HAuCl_4$, and a silver salt, $AgNO_3$, at the surface of seed particles by ascorbic acid [48]. In order to improve mixing in the microfluidic system, the segmented flow principle was applied. While the synthesis of Au/Ag core/shell nanoparticles is carried out at $80\,^{\circ}C$, the Au/Ag/Au core/double shell nanoparticles is synthesized at room temperature. The obtained size distribution of the Au/Ag core/shell and also multishell nanoparticles synthesized by the microflouidic technique is very narrow. In case of Au/Ag core/shell nanoparticles, an average diameter of 20 nm with a distribution half width of $3.8\,$ nm, and for Au/Ag/Au multishell nanoparticles an average diameter of $46\,$ nm with a distribution half width of $7.4\,$ nm are achieved. The optical spectra of the particle solutions exhibited extreme changes with the deposition of each additional metal shell. Due to the changes in their optical properties, the prepared particles are very useful for future sensing applications as well as for labeling in bioanalytics or as nonlinear optical devices

As one spotlight of the increasing interest in biosynthesis of nanoparticles, the microfluidic biosynthesis of Ag nanoparticles in tubular microreactors in the presence of Cacumen Platycladi extract was developed by Liu et al. [51]. The effect of technical parameters (volumetric flow rate, the concentration of the Cacumen Platycladi extract, the inlet mixing pattern) and reactor parameters (reactor materials and inner diameter) on the size distribution of the silver nanoparticles were studied. In order to simulate the profile evolution of the velocity, biomass concentration and temperature within the microreactors, computational fluid dynamics was applied. It was found that, unlike in conventional batch reactors, the interfacial effect between the solid surface and bulk solutions cannot be ignored in microreactors and has important influence on the particle size distribution. Reactor materials with more intense interfacial interaction (coarser surface and larger friction coefficient) with the bulk solutions yield silver nanoparticles with larger average size and wider size distribution. They stated that the relatively coarse surface of the reactor material can provide more sites for nucleation due to its larger superficial area. Nanoparticle deposition on the wall surface increases friction by improving the roughness of the surface. Therefore, materials with rough surfaces are capable of producing a stronger interfacial effect, which then leads to particle formation with larger average size and broader nanoparticle size distribution. In addition, Ag nanoparticles were synthesized with larger average size and broader size distribution. The research revealed the influence of process parameters on the size distribution of Ag nanoparticles in the microfluidic biosynthesis.

2.2.2 Applications

Xu *et al.* [52] reported the fabrication of silver microstructures inserted in a catalytic microreactor. Silver nanostructures were produced by photoreduction (using a femto-second laser) of upright nanoplates and attached nanoparticles and were fabricated inside the microfluidic channel as catalytic active sites for the reduction of 4-nitro-phenol to 4-aminophenol. On-chip catalytic reduction achieved silver microstructures with high catalytic activity. This was monitored by in situ SERS (Surface Enhanced Raman Scattering).

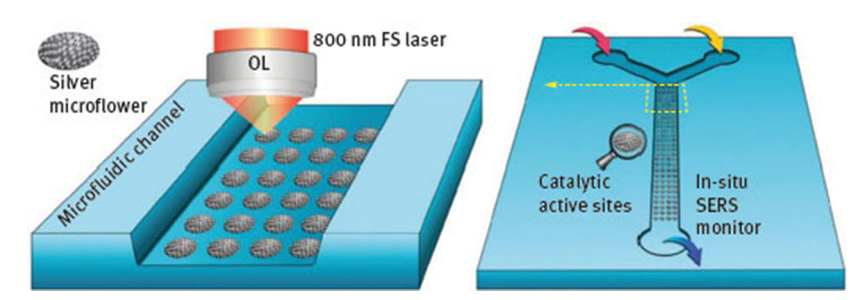


Figure 13: Pictorial representation for the laser fabrication of a Ag microstructure arrays inside a microfluidic chip (reproduced by permission of The Royal Society of Chemistry) [52].

2.3 Palladium

2.3.1 Synthesis

Palladium nanoparticles play a key role as a catalyst in many reactions such as the formation of C–C bonds. Song *et al.* [53] used polymeric as a microfluidic device to produce palladium nanoparticles. The device was fabricated by developing the photoresist SU-8 on a PEEK (polyetherketone) substrate. Five parallel channels were fabricated to scale up the production yield and minimize the mixing volume and dead time. The Pd nanoparticles, when obtained from conventional batch process, had a mean diameter of 3.2 nm with 35% relative standard deviation. The Pd nanoparticles that were produced in microreactor had a lower relative standard deviation of 10% at almost the same mean diameter of 3.0 nm.

A glass capillary microflow reactor system has been used to synthesize palladium nanoparticles by thermal decomposition of palladium acetate ($Pd(OAc)_2$) in diphenyl ether in the presence of poly(benzyl ether) dendron ligands ($PBED\ G_nNH_2$, n=1–3) as a stabilizer [54]. The effects of the hydrodynamic parameter (capillary diameter, velocity, volume flow rate and reaction temperature) and concentration (precursor and stabilizer) on the particle size were investigated. The particle size can be controlled by optimizing the velocity and temperature as well as the ligand/precursor concentration ratio. The particle size is not influenced by the volume flow rate but by the velocity. The reason is that the reaction time is defined by the latter. Unlike batch processes, smaller Pd particles are produced in the microreactor system at low ligand concentrations when the molar ratio of the ligand to metal precursor is kept in the range 1 to 5. As another characteristic of the microreactor synthesis, the concentration of the Pd precursor can be increased (up to 27 mM) with keeping a constant particle size (3.1 \pm 0.2 nm) and a good monodispersity, which is an advantage comparing with batch processes.

Kim *et al.* [55] utilized a droplet-based (water-in-oil droplets) microreactor in order to synthesize Pd nanocrystals with well-controlled shape and size distribution. The applied microreactor was made of polytetrafluoroethylene (PTFE) tube and silica capillaries. The mixing was improved by periodically pinching the PTFE (Figure 14). By manipulating the reducing agent (ascorbic acid) and capping agent (KBr) concentrations, the size and the morphology of the nanoparticles can be tuned. Without KBr, spherical nanoparticles of 4.7 ± 1.2 nm in diameter were formed. While adding KBr in to the droplets in different ratio of Br⁻ /Pd²⁺, nanocubes or nanobars instead of nanospheres were formed. For example, by increasing the molar ratio of Br⁻ /Pd²⁺ from 9.8 to 14.6 and 19.5, the mean average size of the cubes/bars rose from ca. 10 nm (length = 9.0 ± 1.5 nm) to ca. 14 nm (length = 13.4 ± 1.3 nm) and ca. 18 nm (length = 16.9 ± 2.1 nm), with an average aspect ratio of 1.2 (Figure 14) [55].

Shahbazali et al. DE GRUYTER

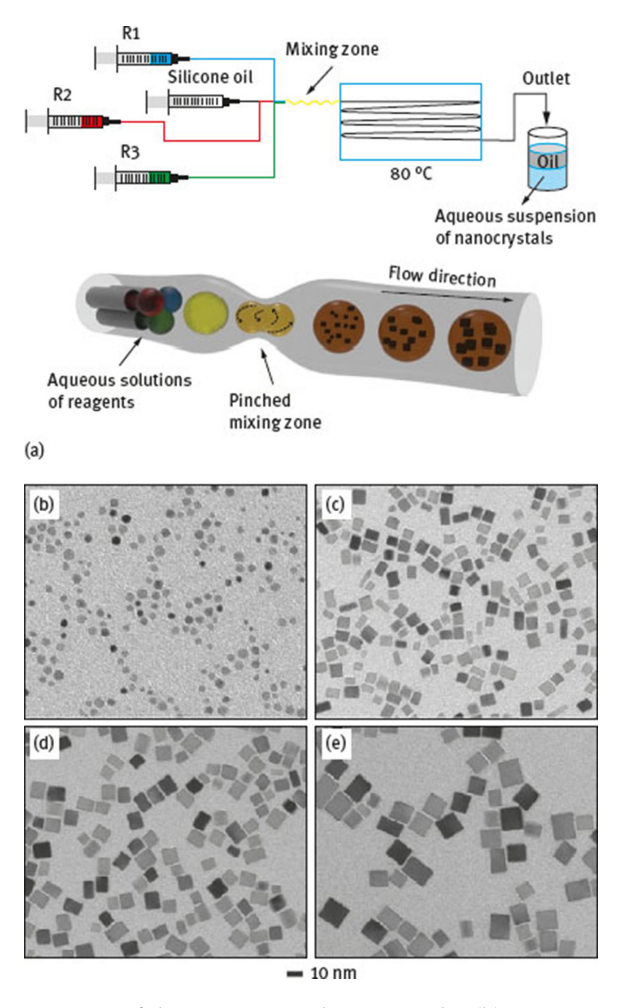


Figure 14: Left: (a) pictorial representation of the experimental setup. Right: (b) TEM image of Pd nanocrytals with controlled size and $Br^-/Pd^{2+}=0$; (c) $Br^-/Pd^{2+}=9.8$; (d) $Br^-/Pd^{2+}=14.6$; and (e) $Br^-/Pd^{2+}=19.5$ (reproduced by permission of Wiley-VCH, Weinheim) [55].

2.3.2 Applications

One of the most important applications of palladium nanoparticles is catalyzing the cross coupling reactions [56]. Ceylan *et al.* applied magnetic silica-coated nanoparticles in an electromagnetic field as a heatable media to perform chemical synthesis [57, 58] (Figure 15). Palladium particles obtained by reductive precipitation of ammonium-bound tetrachloropalladate salts produce nanoparticles which can be used as good catalysts for different Pd-catalytic cross coupling reactions. Only a slight amount of palladium leaching is observed (34 ppm for Suzuki-Miyaura reactions and 100 ppm for Heck reactions).

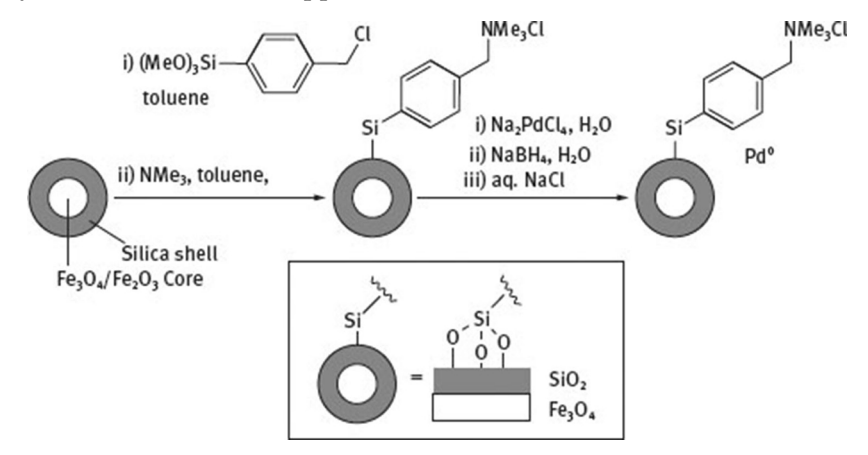


Figure 15: Pictorial representation of the preparation of magnetic nanoparticles doped with Pd° (reproduced by permission of Wiley-VCH, Weinheim) [58].

2.4 Platinum

2.4.1 Synthesis

Platinum nanoparticles, with mean particle size distribution of 1 to 4 nm, were synthesized continuously in microfluidic device by the aid of polyol process [59]. Using the aforementioned process, Baumgard *et al.* [59] showed that the NaOH/Pt ratio (basically the pH value of the synthesis solution) has the most significant influence on the Pt-nanoparticle size distribution. In a more acidic solution, the mean particle size grows to 3.6 nm and demonstrates that the growth reaction has a larger influence on particle formation. However, at a higher NaOH/Pt ratio, the mean particle size decreases to less than 1.7 nm, which specifies that nucleation reaction is more dominant at this condition. Therefore, Baumgard *et al.* designed a two-step microfluidic process in which first Pt-seeds were synthesized in an alkaline medium and an acidic medium was made in a second microreactor. With this two-step process, Pt-nanoparticles were formed with a narrower size distribution [59].

In another work, Lee $et\ al.\ [60]$ demonstrated a microfluidic approach to synthesizing platinum nanoparticles, which were applied to create hierarchical catalyst containing metal-decorated nanoparticles that were assembled into porous microparticles (Figure 16). Applying a spiral silicon-Pyrex microreactor, platinum nanoparticles were produced continuously and coated on to the surface of the magnetic silica nanospheres. The reactants were: amine grafted magnetic core—shell silica suspension; Pt precursor (dipotassium tetrachloroplatinate (II)); and the reducing agents. In order to ensure a single liquid phase reaction, the microreactor is kept at a high pressure of 10 bar and high temperature. At 160 °C with a residence time of 90 s and using ethylene glycol as reducing agent, Pt nanoparticles of about 2.4 ± 0.2 nm are produced and attached to the surface of the magnetic silica nanospheres. These Pt-decorated silica nanospheres are assembled into micron-sized particles by using emulsion templates generated with a microfluidic drop generator. Lastly, in order to study the catalytic reactivity, the assembled particles are introduced into a packed-bed microreactor.

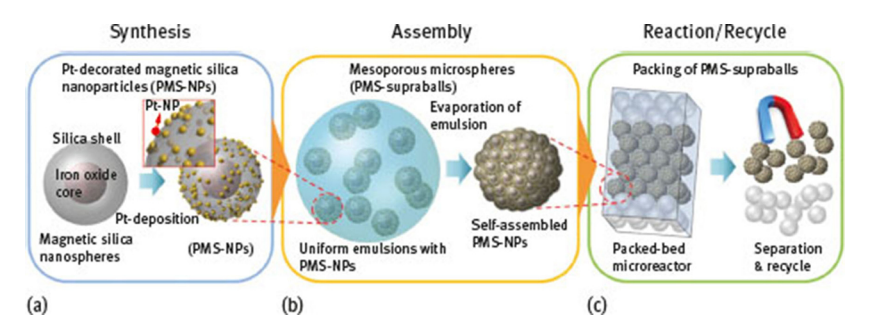


Figure 16: Pictorial representation of the application of a microfluidic system for synthesis, self-assembly, and catalysis with Pt-decorated magnetic silica (PMS) supraballs (reproduced by permission of The Royal Society of Chemistry) [60].

2.4.2 Applications

One of the applications of Pt nanoparticles is to catalyze the hydrogenation of nitrobenzene to aniline. Kataoka *et al.* [61] applied immobilized platinum nanoparticles inside a microreactor in order to catalyze the hydrogenation of nitrobenzene. In order to improve the adsorption and catalytic activity of the nanoparticles, catalytic support layers are offered as a film on the inner wall of the microreactor. Applying an immobilization technique, Pt nanocatalysts demonstrated a good catalytic activity that can be easily regenerated. During 14 hours of continuous experiments and for 50 mM initial nitrobenzene concentration, aniline yields of 92% can be achieved. Table 2 presents a comparison in the activity of catalysts in the microreactor and batch experiments.

Table 2 Comparison of catalyst activity in the microreactor and batch experiments [61].

Catalyst	t [h]	Yields [%]	Yields [%]	
		Aniline	Nitrosobenzene	
Pt/TiO ₂ *	3	30	20	580
Pt/C*	3	60	31	1200
Microreactor	_	92	5.8	3200

Batch experiment, nitrobenzene: 50 mM, $5 \text{ wt } \% \text{ Pt/TiO}_2 \text{ or } 5 \% \text{ Pt/C } 1 \text{ mg}$; IPA: 30 ml; H_2 : 0.1 MPa, 40 °C, 600 rpm.

■ Shahbazali et al. DE GRUYTER

2.5 Copper

2.5.1 Synthesis

The study and comparison of the copper nanoparticle formation between microfluidic and conventional batch processes was reported by Song *et al.* [62]. Compared with results from conventional batch processes, Cu nanoparticles synthesized from microfluidic devices are smaller (8.9 nm vs. 22.5 nm) with narrower size distribution, along with being more stable to oxidation (Figure 17).

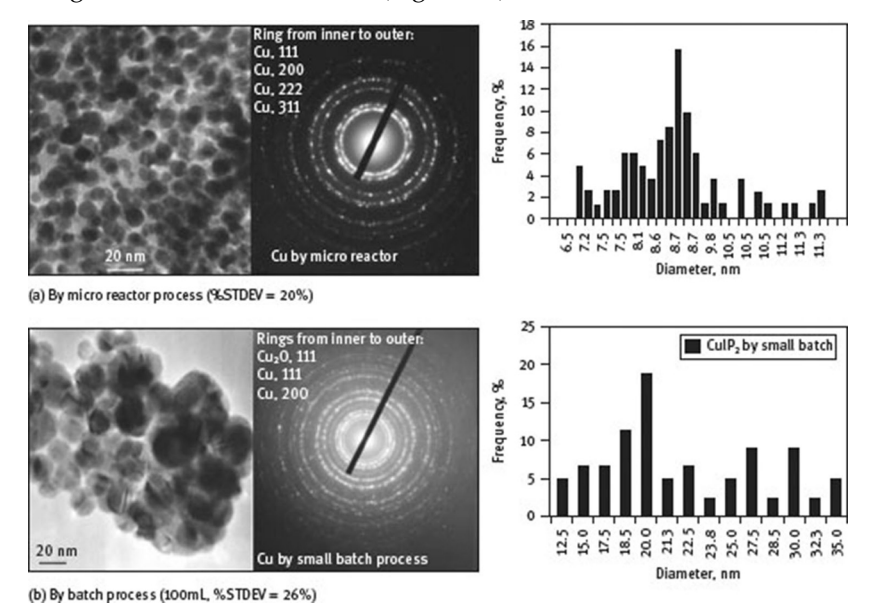


Figure 17: TEM image of Cu nanoparticles synthesized in (a): microreactor process, (b): batch process. In addition, X-ray diffraction analysis and size distribution is given (reprinted with permission from [62]).

Zhang *et al.* reported chemically synthesized copper nanofluids using homemade microfluidic reactors and by using a boiling three-necked flask [63]. The effects of the flow rate of reactants, reactant concentrations and surfactant concentration on the copper particle size and size distribution were studied. Neither of them has much impact on the particle size and size distribution of copper nanoparticles synthesized in microfluidic reactors because of the fast mass diffusion in the microscale dimension. The copper nanoparticle average size was about 3.4 nm with a coefficient of variation of about 22%, whereas the average size distribution of copper nanoparticles formed by batch is 2.7 to 4.9 nm with a coefficient of variation larger than 30%. The synthesis time of copper nanofluids in the microreactor can be reduced as much as one order of magnitude, from about 10 min to about 28 s.

2.5.2 Applications

Compared with Au and Pt, the application of heterogenized Cu calatysts is limited due to their oxidative instability and limited catalyst activity. Cu nanocatalysts were used in the Ullmann-type C–O coupling [64] of potassium phenolate and 4-chloropyridine in a combined microwave (MW) and microflow process.

Benaskar *et al.* [65] developed a process using supported Cu nanocatalyst in an Ullmann etherification reaction. Via the combination of microwave and microflow in one process, the Ullmann-type C–O coupling of potassium phenolate and 4-chloropyridine is performed (Figure 18). By taking advantage of the selective absorption of the microwave energy on the catalyst (by use non-absorbing solvents), yields of up to 80% are attained without substantial catalyst deactivation. The microreactor was packed with beads coated with Cu/TiO₂ and CuZn/TiO₂ catalysts in different segments. By increasing the number of catalyst segments to four, the product yield improves up to 75% in 80 min.

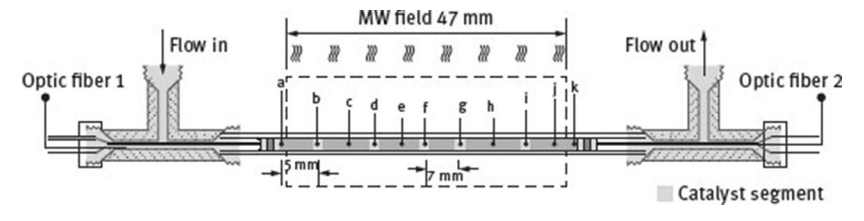


Figure 18: Pictorial representation of the micro-fixed bed reactor and the four positions of catalyst segments (reproduced by permission of Wiley-VCH, Weinheim) [65].

3 Metal nanoparticles in a millifluidic reactor

Recently, in addition to microfluidic devices, the concept of applying millifuidic devices has been introduced in order to synthesize nanoparticles [66–70]. In general, millifluidic devices are referred to as devices that have an internal, transversal scale larger than one millimeter. Millifluidics are easier to fabricate compared to microfluidics; therefore, they are cheaper. Another benefit of using milliflow reactors is that the flow volume is larger than that of microflow reactors, while both microfluidics and millifluidics share main advantages such as precisely defined flow patterns, short residence times and a good mass/heat transfer; yet with different individual qualities. In addition, millifluidic devices can better resist fouling and are easier to interface with typical laboratory devices. Investigating the benefits of applying millifluidics to nanoparticle synthesis, researchers have started to pay attention to them more and more [66–70].

Lately, metal nanoparticles such as gold, silver and copper have been synthesized by applying millifluidics. Li *et al.* studied the size evolution of gold nanoparticles in a millifluidic reactor; they also used numerical simulations to support the experimental data [71]. According to the results, they found particle size can be controlled better when compared to batch reactors. However, the synthesized nanoparticles within the millifluidic channels demonstrated a broad size distribution even at the shortest measured residence time (3.53 s), specifying that both surface growth and reaction kinetics are important in controlling the size and size distribution of nanoparticles [71].

Moreover, Krishna *et al.* [72] employed a millifluidic chip for an in-situ real-time analysis of morphology and dimension-controlled growth of gold nanostructures with a time resolution of 5 ms (Figure 19). Those gold nanoparticles were catalytically active; in order to provide a good application of them, they were applied for the reaction of 4-nitrophenol into 4-aminophenol. For this reaction, applying the gold nanoparticle catalysts with the flow rate of 5 ml/h at T = 298 °C, they could achieve the conversion of 91 %. Without using the gold catalyst, conversion was about 20% [72].

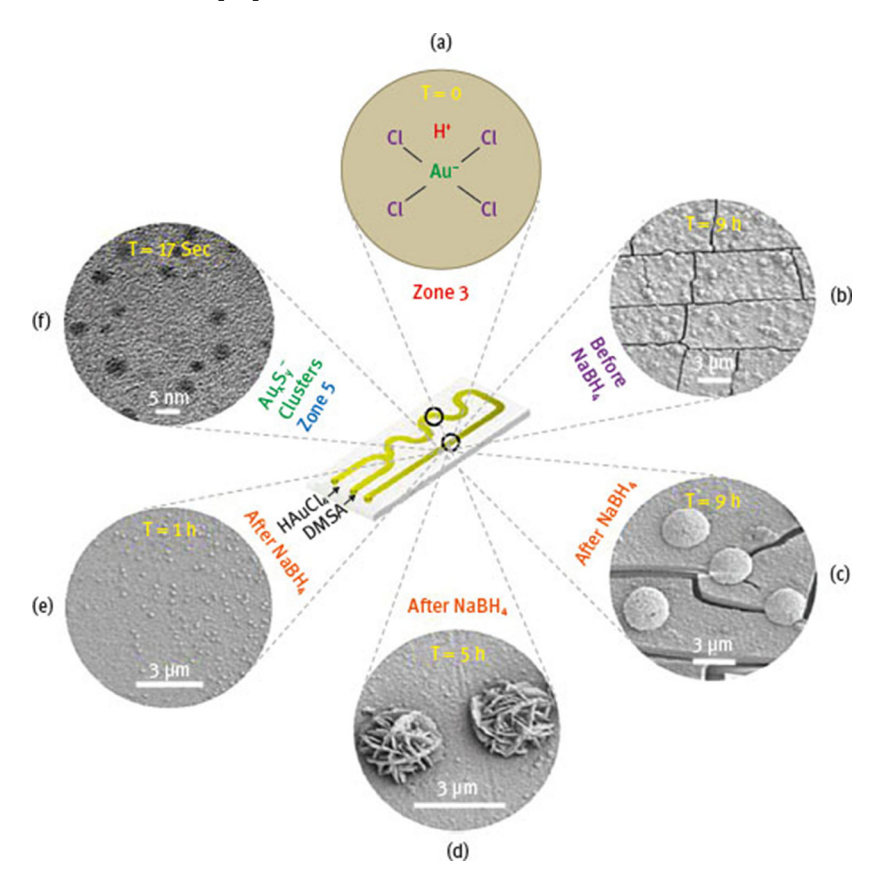


Figure 19: Pictorial representation of time-resolved growth of gold nanostructures within the millifluidic channel (reprinted with permission from [72]);

Jun *et al.* [73] applied a millifluidic mixer to synthesize biocompatible gold nanoparticles (Figure 20). A millifluidic setup enabled them to control the mixing step between a gold salt solution and an ascorbic acid solution at different initial pH; this allows for controlling the final gold nanoparticle sizes (from 3 to 25 nm) with a low polydispersity formed in an aqueous surfactant-free solution [73].

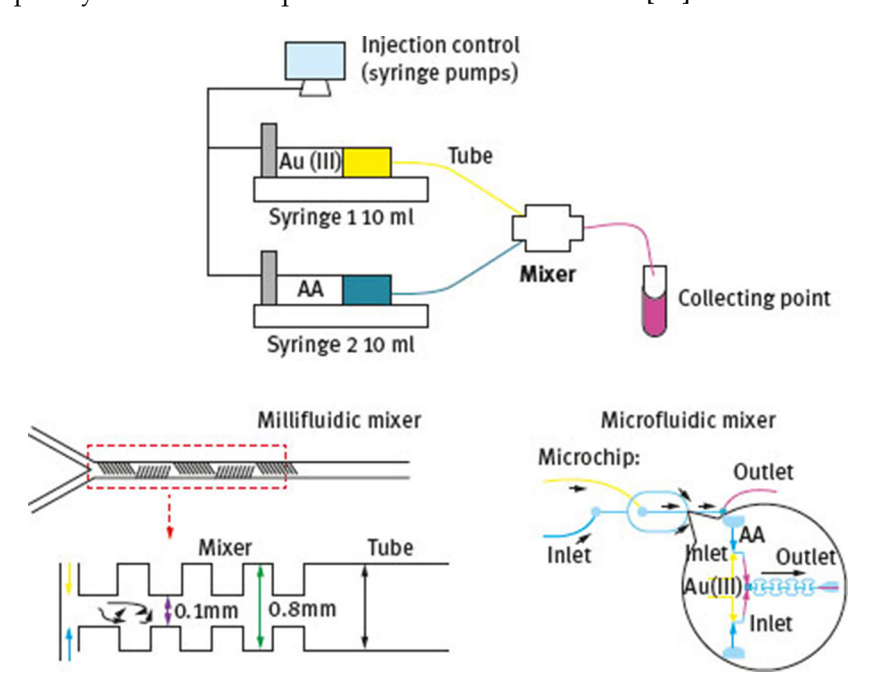
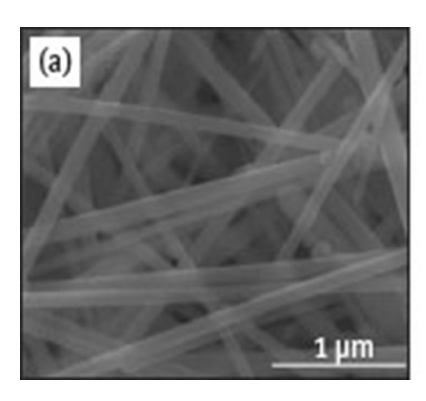


Figure 20: Pictorial representation scheme of the millifluidic mixer (reprinted with permission from [73]);

Gottesman *et al.* synthesized silver nanowires and nanoparticles by a polyol method in a millifluidic reactor and optimized the reaction conditions to get a higher yield of producing nanowires [74]. Besides, they compared their results with the corresponding standard batch reaction. The nanowires that they synthesized in a 30 min reaction time and at a temperature of 198 °C had as its best yield (92% of nanowires) with the average diameter of 71 \pm 2 nm. The batch process yield that they obtained was similar to that from the millifluidic process with the average nanowire diameter of 53 \pm 7 nm (Figure 21) [74].



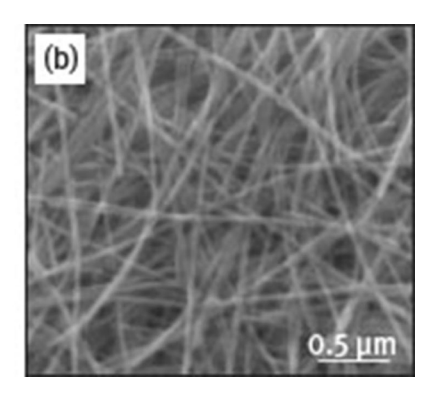


Figure 21: SEM images of silver nanowires synthesized in (a) millifluidics, (b) batch process (reproduced by permission of The Royal Society of Chemistry) [74].

Biswas *et al.* [75] developed a millifluidic platform to synthesize ultra-small copper nanoclusters. Accordingly, by using the millifluid setup, they could achieve low residence time. They also applied numerical simulation and – according to those simulation results – they demonstrated that high flow rates can be produced within the millifluidic reactor owing to the possibility of creating low pressure drops which leads to a decrease in residence times. The low residence times coupled with the use of an effective stabilizing agent such as a bidentate PEGylated surfactant, MPEG, result in a highly stable colloid (stable for more than three months) composed of ultra-small Cu nanoclusters. They also showed that by increasing the flow rate (lowering the residence time) smaller nanoparticles could be produced due to a better control of the growth process at higher flow rates [75] (Figure 22).

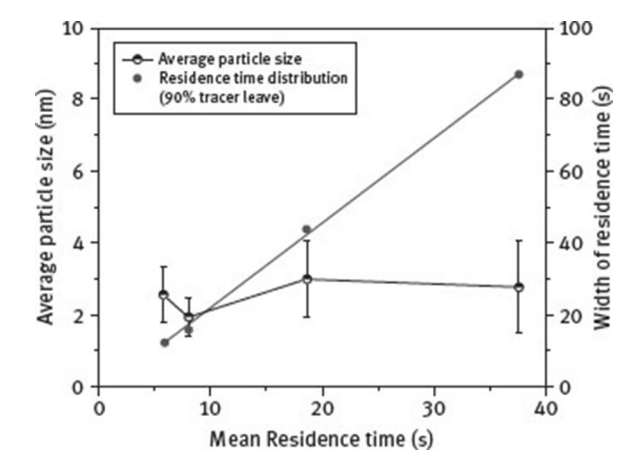


Figure 22: The analysis of size and size distribution of Cu nanoclusters with mean residence times within the millifluidic reactor (reproduced by permission of Wiley-VCH, Weinheim) [75].

In view of all these and other related developments achieved during the past two years, it can be summarized that millifluidic devices have become attractive for the synthesis of nanomaterials because they present growing potentials and the possibility of future applications in the field. Nevertheless, here is still much room open for thorough investigations for applications in nanomaterial synthesis.

4 Outlook – metal nanoparticles generated in flow and used in situ

The application of flow chemistry can offer the possibility for the *in situ* generation of nanomaterials. Due to the short residence time scales of microfluidics, the unstable intermediates can be generated in flow. In this context, Yoshida $et\ al.$ applied the flash chemistry concept [76], which utilizes in-flow generated high-energy intermediates for ultrafast reactions, towards the creation of new generations of unstable catalysts. These unstable reactive catalysts are generated fast and consumed in a later reaction before they decompose. With such an approach, Nagaki $et\ al.$ [77] prepared a new generation of a highly reactive Pd catalyst for the Suzuki-Miyaura coupling [78] by using a flow microreactor (Figure 23). Since there are hardly any available examples of $in\ situ$ generated heterogeneous nanocatalysts in microfluidics, the work of Nagaki $et\ al.$ [77] is presented in this part, although their reactive catalyst is homogeneous. This catalyst species was generated from the fast mixing of the precursors $[Pd(OAc)_2]$ (1 mol %) and $t\ Bu_3P$ (1 mol %) in a micromixer. The outcoming flow mixture is then directly injected into a reaction section in which the Suzuki-Miyaura reaction mixture flows (residence time: 0.65 s).

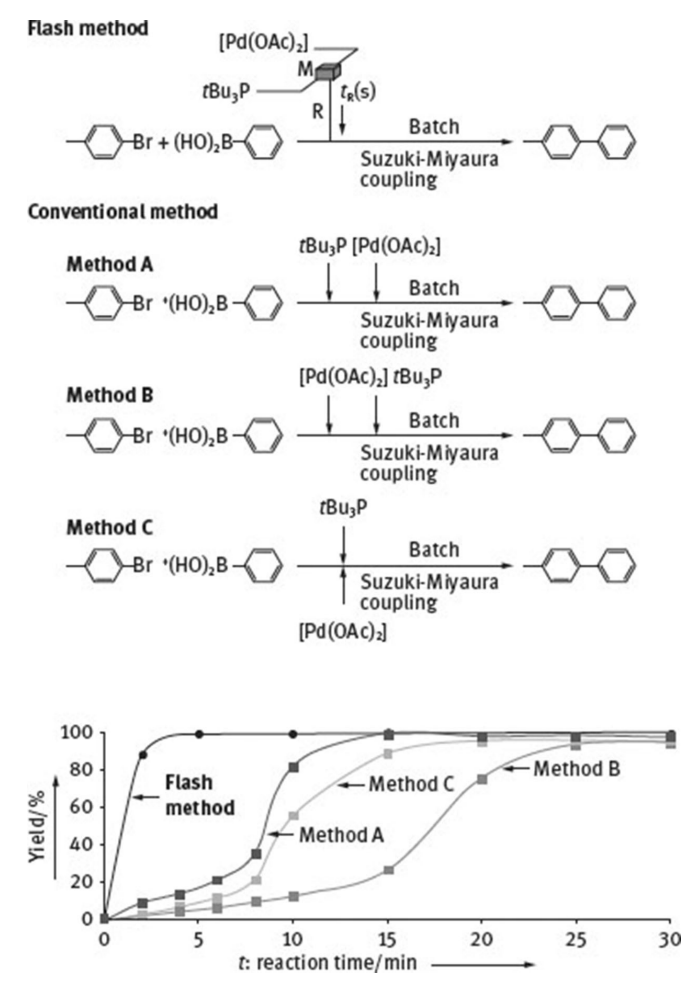


Figure 23: Suzuki–Miyaura coupling of p-bromotoluene and phenylboronic acid in the presence of KOH catalyzed by $[Pd(OAc)_2]$ –t Bu₃P. Flash method: premixed catalyst precursor solutions of $[Pd(OAc)_2]$ and t Bu₃P; method A: separate e of t Bu₃P and t Bu₃P and t Bu₃P (1 mol %) with 10 s delay; method C: parallel feed of non-premixed t Bu₃P (reproduced by permission of Wiley-VCH, Weinheim) [77].

This processing, called "flash method", is compared to three alternative injection schemes (methods A–C) that introduce the two catalyst precursors separately, either in a serial or parallel fashion directly into the reaction mixture. Accordingly, such injected catalysts exhibit a much slower reaction performance than the unstable, highly active flash catalyst.

The difference in reaching reaction completion ranges from about 3 min (flash) to about 15 min (method A) to about 30 min (method B).

This homogeneous catalytic reaction example with an unstable catalytic intermediate has a heterogeneous counterpart. Jamal $et\ al.$ [79] combined the synthesis of gold nanoparticles with their immobilization in a microreactor in order to apply it in a catalytic organic reaction. Gold nanoparticles produced in this way have very narrow size distribution (1–3 nm) and are immobilized into the inner volume of functionalized silica microcapillaries, which then constitute the catalytic microreactor. This example can be considered as an outlook of a promising process that combines the advantages of microfluidic devices to synthesize nanoparticles and using them $in\ situ$ as catalysts in organic reactions.

5 Conclusions

This chapter aims to cover recent achievements on metal nanoparticles, which are produced in continuous flow (micro and millifluidics) devices, and their catalytic applications in organic flow-based synthesis. The significantly reduced diffusion distance (and similar benefits in convection) in microfluidic systems provides strongly improved mixing and heat transfer. Miniaturization also allows the realization of compact formats of complex integrated flow schemes, e.g. with multiple injection points. Two prime enablers stem from those two benefits – first, reduced and thus kinetically matched residence times and, second, decoupling of elementary processes (each under optimal conditions) by serial injection and reaction treatments of reactants. This allows

Automatically generated rough PDF by *ProofCheck* from River Valley Technologies Ltd

metal nanoparticles to be synthesized with controlled size, shape and size distribution. In the field of organic chemistry, metal nanoparticles produced in this way can be applied as catalysts. The same applies to flow chemistry as part of organic chemistry. The joined benefits of flow chemistry and catalytic nanoparticles can remarkably enhance the reaction performance, e.g. in terms of minimizing the reaction time and improving the yield.

Acknowledgment

We kindly acknowledge the European Research Council for the Advanced Grant on "Novel Process Windows" No. 267443.

Contents of this chapter were taken from a previous paper of ours, published as "Nanotechnol. Rev. 2014, 3(1), 65–86", and updated with some more information. We acknowledge that de Gruyter publishers allowed us to use this material.

This article is also available in: Saha, Catalytic Reactors. De Gruyter (2015), isbn 978-3-11-033296-4.

References

- [1] Caruso F, Caruso A, Möhwald H. Nanoengineering of inorganic and hybrid hollow spheres by colloidal templating. Science 1998, 282, 1111–1114.
- [2] Ferreira AJ, Cemlyn-Jones J, Cordeiro CR. Nanoparticles, nanotechnology and pulmonary nano-toxicology Nanopartículas, nanotecnologia e nanotoxicologia pulmonary. Rev. Port Pneumol. 2013, 19, 28–37.
- [3] Salata OV. Applications of nanoparticles in biology and medicine. J. Nanobiotechnol. 2004, 2, 3–6.
- [4] Coe S, Woo W, Bawendi M, Bulovic V. Electroluminescence from single monolayers of nano-crystals in molecular organic devices. Nature 2002, 420, 800–803.
- [5] Bruchez M, Moronne M, Gin P, Weiss S, Alivisatos A. Semiconductor nanocrystals as fluorescent biological labels. Science 1998, 281, 2013–2016.
- [6] Xuan J, Jia X, Jiang L, Abdel-Halim ES, Zhu J. Gold nanoparticle-assembled capsules and their application as hydrogen peroxide biosensor based on hemoglobin. Bioelectrochemistry 2012, 84, 32–37.
- [7] Cushing B, Kolesnichenko V, O'Connor C. Recent Advances in the Liquid-Phase Syntheses of Inorganic Nanoparticles. Chem. Rev. 2004, 104, 3893–3946.
- [8] Trewyn B, Slowing I, Giri S, Chen H, Lin V. Synthesis and Functionalization of a Mesoporous Silica Nanoparticle Based on the Sol–Gel Process and Applications in Controlled Release. Acc. Chem. Res. 2007, 40, 846–853.
- [9] Eastoe], Hollamby M, Hudson L. Recent advances in nanoparticle synthesis with reversed micelles. Adv. Colloid Interface Sci. 2006, 128–130, 5–15.
- [10] Rassy H, Belamie E, Livage J, Coradin T. Onion phases as biomimetic confined media for silica nanoparticle growth. Langmuir 2005, 21, 8584–8587.
- [11] Marre S, Jensen K. Synthesis of micro and nanostructures in microfluidic systems. Chem. Soc. Rev. 2010, 39, 1183–1202.
- [12] Zhao C, He L, Qiao S, Middelberg A. Nanoparticle synthesis in microreactors. Chem. Eng. Sci. 2011, 66, 1463–1479.
- [13] Luo G, Du L, Wang Y, Lu Y, Xu J. Controllable preparation of particles with microfluidics. Particuology 2011, 9, 545–558.
- [14] Hung L, Lee A. Microfluidic Devices for the Synthesis of Nanoparticles and Biomaterials. J. Med. Biol. Eng. 2007, 27, 1–6.
- [15] DeMello A. Control and detection of chemical reactions in microfluidic systems. Nature 2006, 442, 394–402.
- [16] Jensen K. Microreaction engineering is small better?. Chem. Eng. Sci. 2001, 56, 293–303.
- [17] Krishnadasan S, Tovilla J, Vilar R, DeMello A, DeMello J. On-line analysis of CdSe nanoparticle formation in a continuous flow chip-based microreactor. J. Mater. Chem. 2004, 14, 2655–2660.
- [18] Sounart T, Safier P, Voigt J, Hoyt J, Tallant D, Matzke C, Michalske T. Spatially-resolved analysis of nanoparticle nucleation and growth in a microfluidic reactor. Lab Chip 2007, 7, 908–915.
- [19] Abou-Hassan A, Sandre O, Cabuil V. Microfluidics in Inorganic Chemistry. Angew. Chem. Int. Ed. 2010, 49, 6268–6286.
- [20] Veiseh O, Sun C, Gunn J, Kohler N, Gabikian P, Lee D, Bhattarai N, Ellenbogen R, Sze R, Hallahan A, Olson J, Zhang M. Optical and MRI multifunctional nanoprobe for targeting gliomas. Nano Lett. 2005, 5, 1003–1008.
- [21] Park J, Saffari A, Kumar S, Gunther A, Kumacheva E. Microfluidic Synthesis of Polymer and Inorganic Particulate Materials. Annu. Rev. Mate.r Res. 2010, 40, 415–443.
- [22] Cottam B, Krishnadasan S, DeMello A, DeMello J, Shaffer M. Accelerated synthesis of titanium oxide nanostructures using microfluidic chips. Lab Chip 2007, 7, 167–169.
- [23] Kumar K, Nightingale A, Krishnadasan S, Kamaly N, Wylenzinska-Arridge M, Zeissler K, Branford W, Ware E, DeMello A, DeMello J. Direct synthesis of dextran-coated superparamagnetic iron oxide nanoparticles in a capillary-based droplet reactor. J. Mater. Chem. 2012, 22, 4704–4708.
- [24] Winterton J, Myers D, Lippmann J, Pisano A, Doyle F. A novel continuous microfluidic reactor design for the controlled production of high-quality semiconductor nanocrystals. J. Nanoparticle Res. 2008, 10, 893–905.
- [25] Abdelhady A, Afzaal M, Malik M and O'Brien P. Flow reactor synthesis of CdSe, CdSe, CdSe/CdS and CdSeS nanoparticles from single molecular precursor(s). J. Mater. Chem. 2011, 21, 18768–18775.

- [26] Wagner J, Köhler M. Continuous synthesis of gold nanoparticles in a microreactor. Nano Lett. 2005, 5, 685–691.
- [27] Lin X, Terepka A, Yang H. Synthesis of silver nanoparticles in a continuous flow tubular microreactor. Nano Lett. 2004, 4, 2227–2232.
- [28] Pacławski K, Streszewski B, Jaworski W, Luty-Błocho M, Fitzner K. Gold nanoparticles formation via gold(III) chloride complex ions reduction with glucose in the batch and in the flow microreactor systems. Colloids and Surfaces A: Physicochem. Eng. Aspects 2012, 413, 208–215.
- [29] Wang H, Li X, Uehara M, Yamaguchi Y, Nakamura H, Miyazaki M, Shimizu H, Maeda H. Continuous synthesis of CdSe–ZnS composite nanoparticles in a microfluidic reactor. Chem. Comm. 2004, 48–49.
- [30] Wagner J, Tshikhudo TR, Kohler JM. Microfluidic generation of metal nanoparticles by borohydride reduction. Chem. Eng. J. 2008, 135S, S104–S109.
- [31] Shestopalov, Tice JD, Ismagilov RF. Multi-step synthesis of nanoparticles performed on millisecond time scale in a microfluidic droplet-based system. Lab Chip 2004, 4, 316–321.
- [32] Eder RJP, Schrank S, Besenhard MO, Roblegg E, Gruber-Woelfler H, Khinast J.G. Continuous Sonocrystallization of Acetylsalicylic Acid (ASA): Control of Crystal Size. Growth Des. 2012, 12, 4733–4738.
- [33] DeMello J, DeMello A. Microscale reactors: nanoscale products. Lab Chip 2004, 4, 11N-15N.
- [34] Daniel M, Astruc D. Gold Nanoparticles: Assembly, Supramolecular Chemistry, Quantum-Size-Related Properties, and Applications toward Biology, Catalysis, and Nanotechnology. Chem. Rev. 2004, 104, 293–346.
- [35] Köhler J, Wagner J, Albert J. Formation of isolated and clustered Au nanoparticles in the presence of polyelectrolyte molecules using a flow-through Si chip reactor. J. Mater. Chem. 2005, 15, 1924–1930.
- [36] Luty-Błocho M, Fitzner K, Hessel V, Löb P, Maskos M, Metzke D, Pacławski K, Wojnicki M. Synthesis of gold nanoparticles in an interdigital micromixer using ascorbic acid and sodium borohydride as reducers. Chem. Eng. J. 2011, 171, 279–290.
- [37] Nightingale A, DeMello J. Segmented Flow Reactors for Nanocrystal Synthesis. Adv. Mater., doi: 10.1002/adma.201203252.
- [38] Cabeza V, Kuhn S, Kulkarni A, Jensen K. Size-controlled flow synthesis of gold nanoparticles using a segmented flow microfluidic platform. Langmuir 2012, 28, 7007–7013.
- [39] Boleininger J, Kurz A, Reuss V, Sonnichsen C. Microfluidic continuous flow synthesis of rodshaped gold and silver nanocrystals. Phys. Chem. Chem. Phys. 2006, 8, 3824–3827.
- [40] Bullen C, Latter M, D'Alonzo N, Willis G, Raston C. A seedless approach to continuous flow synthesis of gold nanorods. Chem. Commun. 2011, 47, 4123–4125.
- [41] Duraiswamy S, Khan S. Droplet-Based Microfluidic Synthesis of Anisotropic Metal Nanocrystals. Small 2009, 5, 2828–2834.
- [42] Gomez L, Sebastian V, Irusta S, Ibarra A, Arruebo M, Santamaria J. Scaled-Up Production of Plasmonic Nanoparticles Using Microfluidics: From Metal Precursors to Functionalized and Sterilized Nanoparticles. Lab Chip 2014, 14, 325.
- [43] Abahmane L, Köhler J, Groß G. Gold-Nanoparticle-Catalyzed synthesis of propargylamines: the traditional A3-multicomponent reaction performed as a two-step flow process. Chem. Eur. J. 2011, 17, 3005–3010.
- [44] Gross E, Liu J, Toste F, Somorjai G. Control of selectivity in heterogeneous catalysis by tuning nanoparticle properties and reactor residence time. Nature Chemistry 2012 4, 947–952.
- [45] Gómez-de Pedro S, Lopes D, Miltsov S, Izquierdo D, Alonso-Chamarro J, Puyol M. Optical Microfluidic System Based on Ionophore Modified Gold Nanoparticles for the Continuous Monitoring of Mercuric Ion. Sensors and Actuators B 2014, 194, 19–26.
- [46] He S, Kohira T, Uehara M, Kitamura T, Nakamura H, Miyazaki M, Maeda H. Effects of interior wall on continuous fabrication of silver nanoparticles in microcapillary reactor. Chem. Lett. 2005, 34, 748–749.
- [47] Ravi Kumar D, Prasad B, Kulkarni A. Segmented flow synthesis of Ag nanoparticles in spiral microreactor: Role of continuous and dispersed phase. Chem. Eng. J. 2012, 192, 357–368.
- [48] Knauer A, Thete A, Li S, Romanus H, Csáki A, Fritzsche W, Köhler J. Au/Ag/Au double shell nanoparticles with narrow size distribution obtained by continuous micro segmented flow synthesis. Chem. Eng. J. 2011, 166, 1164–1169.
- [49] Yang Y, Shi J, Kawamura G, Nogami M. Preparation of Au–Ag, Ag–Au core–shell bimetallic nanoparticles for surface-enhanced Raman scattering. Scripta Mater. 2008, 58, 862–865.
- [50] Rodriguez-Gonzalez B, Burrows A, Watanabe M, Kiely C, Liz-Marzán L. Multishell bimetallic AuAg nanoparticles: synthesis, structure and optical properties. J. Mater. Chem. 2005 15, 17, 1755–1759.
- [51] Liu H, Huang J, Sun D, Lin L, Lin W, Li J, Jiang X, Wu W, Li Q. Microfluidic biosynthesis of silver nanoparticles: Effect of process parameters on size distribution. Chem. Eng. J. 2012, 209, 568–576.
- [52] Xu B, Zhang R, Liu X, Wang H, Zhang Y, Jiang H, Wang L, Ma Z, Ku J, Xiao F, Sun H. On-chip fabrication of silver microflower arrays as a catalytic microreactor for allowing in situ SERS monitoring. Chem. Commun. 2012, 48, 1680–1682.
- [53] Song Y, Kumar C, Hormes J. Synthesis of palladium nanoparticles using a continuous flow polymeric micro reactor. J. Nanosci. Nanotech. 2004, 4, 788–793.
- [54] Torigoe K, Watanabe Y, Endo T, Sakai K, Sakai H, Abe M. Microflow reactor synthesis of palladium nanoparticles stabilized with poly(benzyl ether) dendron ligands. J. Nanopart. Res. 2010, 12, 951–960.
- [55] Kim Y, Zhang L, Yu T, Jin M, Qin D, Xia Y. Droplet-Based Microreactors for Continuous Production of Palladium Nanocrystals with Controlled Sizes and Shapes. Small 2013, 9, No. 20, 3462–3467.
- [56] Noël T, Buchwald S. Cross-coupling in flow. Chem. Soc. Rev., 2011, 40, 5010–5029.
- [57] Ceylan S, Friese C, Lammel C, Mazac K, Kirschning A. Inductive Heating for Organic Synthesis by Using Functionalized Magnetic Nanoparticles Inside Microreactors. Angew. Chem. Int. Ed. 2008, 47, 8950–8953.
- [58] Ceylan S, Coutable L, Wegner J, Kirschning A. Inductive Heating with Magnetic Materials inside Flow Reactors. Chem. Eur. J. 2011, 17, 1884–1893.
- [59] Baumgard J, Vogt A, Kragl U, Jähnisch K, Steinfeldt N. Application of microstructured devices for continuous synthesis of tailored platinum nanoparticles. Chem. Eng. J. 2013, 227, 137–144.
- [60] Lee S, Liu X, Cabeza V, Jensen K. Synthesis, assembly and reaction of a nanocatalyst in microfluidic systems: a general platform. Lab Chip 2012, 12, 4080–4084.

Automatically generated rough PDF by ProofCheck from River Valley Technologies Ltd

- [61] Kataoka S, Takeuchi Y, Harada A, Takagi T, Takenaka Y, Fukaya N, Yasuda H, Ohmori T, Endo A. Microreactor containing platinum nanoparticles for nitrobenzene hydrogenation. Appl. Catal. A: Gen. 2012, 427–428, 119–124.
- [62] Song Y, Doomes E, Prindle J, Tittsworth R, Hormes J, Kumar C. Investigation into sulfobetaine-stabilized Cu nanoparticle formation: toward development of a microfluidic synthesis. J. Phys. Chem. B 2005, 109, 9330–9338.
- [63] Zhang Y, Jiang W, Wang L. Microfluidic synthesis of copper nanofluids. Microfluid Nanofluid 2010, 9, 727–735.
- [64] Monnier F, Taillefer M. Catalytic C-C, C-N, and C-O Ullmann-Type Coupling Reactions. Angew. Chem. Int. Ed. 2009, 48, 6954–6971.
- [65] Benaskar F, Patil N, Rebrov E, Ben-Abdelmoumen A, Meuldijk J, Hulshof L, Hessel V, Schouten J. Micro/Milliflow Processing with Selective Catalyst Microwave Heating in the Cu-Catalyzed Ullmann Etherification Reaction: A μ2-Process" ChemSusChem. doi: 10.1002/c-ssc.201200504, 2012.
- [66] Testouri A, Arriaga L, Honorez C, Ranft M, Rodrigues J, van der Net A, Lecchi A, Salonen A, Rio E, Guillermic R, Langevin D, Drenckhan W. Generation of porous solids with well-controlled morphologies by combining foaming and flow chemistry on a Lab-on-a-Chip. Colloids and Surfaces A: Physicochem. Eng. Aspects 2012, 413, 17–24.
- [67] Tadmouri R, Romano M, Guillemot L, Mondain-Monval O, Wunenburger R, Leng J. Soft Matter. 2012, 8, 10704–10711.
- [68] Li Y, Yamane D, Li S, Biswas S, Reddy R, Goettert J, Nandakumar K, Kumar C. Geometric optimization of liquid—liquid slug flow in a flow-focusing millifluidic device for synthesis of nanomaterials. Chem. Eng. J. 2013, 217, 447–459.
- [69] Kitson P, Rosnes M, Sans V, Dragone V and Cronin L. Configurable 3D-Printed millifluidic and microfluidic 'lab on a chip' reactionware devices. Lab Chip 2012, 12, 3267–3271.
- [70] Lohse S, Eller J, Sivapalan S, Plews M, Murphy C. ACS Nano 2013, 7 (5), 4135–4150.
- [71] Li Y, Sanampudi A, Reddy V, Biswas S, Nandakumar K, Yemane D, Goettert J, Kumar C. Size Evolution of Gold Nanoparticles in a Millifluidic Reactor. ChemPhysChem 2012, 13, 177–182.
- [72] Krishna K, Navin C, Biswas S, Singh V, Ham K, Bovenkamp G, Theegala C, Miller J, Spivey J, Kumar C. Millifluidics for Time-resolved Mapping of the Growth of Gold Nanostructures. J. Am. Chem. Soc. 2013, 135, 5450–5456.
- [73] Jun H, Fabienne T, Florent M, Coulon P, Nicolas M, Olivier S. Understanding of the Size Control of Biocompatible Gold Nanoparticles in Millifluidic Channels. Langmuir 2012, 28, 15966–15974.
- [74] Gottesman R, Tangy A, Oussadon I, Zitoun D. Silver nanowires and nanoparticles from a millifluidic reactor: application to metal assisted silicon etching. New J. Chem. 2012, 36, 2456–2459.
- [75] Biswas S, Jeffrey T, Miller J, Li Y, Nandakumar K, Kumar C. Developing a Millifluidic Platform for the Synthesis of Ultrasmall Nanoclusters: Ultrasmall Copper Nanoclusters as a Case Study. Small 2012, 8, 5, 688–698.
- [76] Yoshida J. Flash Chemistry: Fast Organic Synthesis in Microsystems. Wiley–Blackwell, Chichester, 2008.
- [77] Nagaki A, Takabayashi N, Moriwaki Y, Yoshida J. Flash Generation of a Highly Reactive Pd Catalyst for Suzuki–Miyaura Coupling by Using a Flow Microreactor. Chem. Eur. J. 2012, 18, 11871–11875.
- [78] Kotha S, Lahiri K, Kashinath D. Recent applications of the Suzuki–Miyaura cross-coupling reaction in organic synthesis. Tetrahedron 2002, 58, 9633–9695.
- [79] Jamal F, Jean-Sebastien G, Mael P, Edmond P, Christian R. Gold nanoparticle synthesis in microfluidic systems and immobilization in microreactors designed for the catalysis of fine organic reactions. Microsyst. Technol. 2012, 18, 151–158.